J. Phys.: Condens. Matter **20** (2008) 184004 (8pp) doi:10.1088/0953-8984/20/18/184004

Thiol-capped gold: from planar to irregular surfaces

C Vericat, G A Benitez, D E Grumelli, M E Vela and R C Salvarezza

Instituto de Investigaciones Fisicoquímicas Teóricas y Aplicadas (INIFTA), Universidad Nacional de La Plata—CONICET, Sucursal 4 Casilla de Correo 16 (1900) La Plata, Argentina

Received 4 September 2007, in final form 21 December 2007
Published 17 April 2008
Online at stacks.iop.org/JPhysCM/20/184004

Abstract

Thiol-capped metals, in particular gold, have a wide range of technological applications, especially for building systems by bottom-up methods. In most cases, stability of the organic film during exposure to ambient conditions and/or to electrolyte solutions is a crucial requirement. In this work we discuss the stability of butanethiol self-assembled monolayers (SAMs) on planar, nanocurved and irregular Au surfaces against both air exposure and electrodesorption in aqueous media. We have found a slower rate of air oxidation and increased stability against electrodesorption for butanethiol monolayers on highly irregular Au surfaces as compared to those on planar surfaces. The increased stability of SAMs on highly irregular surfaces is promising because desorption and degradation seriously limit their application in nanotechnology.

1. Introduction

Organic molecular films have a broad field of applications in molecular electronics, and also as electrochromic devices, sensors, biomolecular chips, resists for soft lithography, and surface active agents for modifying the properties of solid surfaces, among others [1–6]. Self-assembled monolayers (SAMs) of thiols on metals and semiconductors are the most popular type of organic molecular films [2, 7]. Thiol SAMs represent an easy path to link inorganic, organic and biological materials to metal surfaces [1]. The sulfur atom of the molecule links a hydrocarbon chain of variable length to the metal surface through a covalent bond, while van der Waals forces between neighboring molecules contribute to stabilize the structure [8]. The thiol terminal group confers specific properties to the surface, and can also be used to anchor different molecules, biomolecules, or nanostructures by weak interactions or covalent bonds [2, 6]. SAMs of thiols can be prepared on different metals and semiconductor surfaces, such as Au, Ag, Cu, Pd, Pt, Ni, and GaAs, either from solution or by vapor phase deposition [9]. However, Au is the preferred substrate for solution preparation, since oxide-free, clean, flat surfaces can be easily obtained in ambient conditions. The strong S–Au bond and the interactions among hydrocarbon chains yield dense, crystalline alkanethiol monolayers, both in gas and liquid phases [7–9].

Most of our information about thiol SAM structure and bonding on Au is related to planar surfaces, like single crystals or evaporated films on substrates such as glass, silicon or mica. However, in the last years, a great interest has arisen for thiol SAMs on Au nanoparticles (AuNP) [2, 10, 11], which have a wide range of applications, from electronics to medicine [12–14]. Metal NP can be obtained by simple 'wet chemistry' synthetic methods that usually involve thiol as one of the reactants, which forms a protective cap that reduces NP growth and avoids aggregation [10, 15]. At the same time, different thiols can be used to anchor a wide variety of molecules and biomolecules [16], thus conferring specific functionalities to the NP surface.

On the other hand, high area functionalized metal surfaces are important to improve the performance of sensors, biosensors and optical devices by increasing either the optical or electrical signals with respect to those of a planar surface due to an area increase [6, 17]. Also, these metal surfaces are promising in the fields of electrocatalysis and bioelectrocatalysis. As in the case of planar surfaces and NP, thiols have been used to anchor different molecules and biomolecules to these high area irregular surfaces by using covalent bonds or weak interactions. Thiol-covered nanostructured high area Au surfaces have also been investigated because they exhibit properties that do not depend linearly on the area, like super-hydrophobicity and super-hydrophilicity [18], and the surface enhanced Raman scattering (SERS) effect [19].

In most technological applications the stability of the organic film during exposure to ambient conditions and/or to

electrolyte solutions is a crucial requirement. It has been reported that the resistance of thiol in these environments depends on the characteristics of the gold substrate [20]. Therefore, this point deserves further investigation.

In this work we have compared the stability of butanethiol self-assembled monolayers (SAMs) on planar, nanocurved and irregular Au surfaces against air exposure and also to aqueous media. After a brief overview about SAM organization on the different substrates and on their applications, we report new experimental results showing that thiol monolayers exhibit greater stability in both environments (air and aqueous solutions) in the case of highly irregular Au surfaces as compared to planar surfaces. The increased stability of SAMs on highly irregular surfaces is promising because desorption and degradation seriously limit their applications in nanotechnology.

2. Experimental details

Three different types of samples were prepared for the experiments:

(a) Thiol SAM on planar gold. Flame annealed substrates (purchased from Arrandees™), consisting of vapor deposited gold films (250 ± 50 nm in thickness) on a thin layer of chromium supported on glass were used. These polycrystalline substrates exhibit large grains with atomically smooth terraces separated by steps of monatomic height [21]. Butanethiol self-assembled monolayers were prepared by immersing the substrates in 50 μM butanethiol ethanolic solutions for 24 h.

(b) Curved gold surfaces. Butanethiol-covered gold nanoparticles (AuNP) 3 nm in size prepared by the Brust method were used [22]. Highly oriented pyrolytic graphite (HOPG) substrates were immersed in a 0.3 mg ml^{-1} butanethiol-capped AuNP-containing hexane solution for 30 min to form gold-coated carbon surfaces [23].

(c) Highly irregular gold surfaces. Nanostructured gold substrates were prepared following the procedure described in [24]. Briefly, polycrystalline gold plates were anodized in 0.5 M H_2SO_4 solution for 5 min at 2.4 V (versus a saturated calomel electrode (SCE) reference) in a conventional 3-electrode electrochemical cell. This anodization process results in the formation of a thick hydrous gold oxide. Immediately afterward the potential was cathodically swept at 0.025 V s^{-1} and held at −0.5 V for 5 min to electroreduce the thick gold oxide and thus obtain a highly irregular gold surface (black gold) with a real surface area ≈50 times greater than the starting gold surface. The real surface area of the resulting irregular metallic surface was voltammetrically measured in the same 3-electrode cell and electrolyte by calculating the charge related to the AuO → Au phase change, i.e. the electroreduction charge [24]. For this purpose the potential applied to the Au surface in contact to the electrolyte solution was ramped at a constant rate, while recording the current (voltammetry). The real surface area was then calculated by measuring the charge of the AuO monolayer electroreduction peak and by considering that 440 μC correspond to 1 cm^2 [24]. Butanethiol self-assembled monolayers were prepared by immersing the freshly prepared substrates in 50 μM butanethiol ethanolic solutions for 24 h.

In all cases, the thiol-covered substrates were removed from the solution, carefully rinsed with the solvent (ethanol for planar and irregular gold surfaces and hexane for the Au NP supported on HOPG) and finally dried under nitrogen to be characterized by scanning tunneling microscopy (STM), x-ray photoelectron microscopy (XPS) or by electrochemical techniques.

STM imaging was made in the constant current mode in air with a Nanoscope IIIa microscope from Veeco Instruments (Santa Barbara, CA). Commercial Pt–Ir tips were used, which were insulated with Apiezon wax for ECSTM. Typical tunneling currents and bias voltages were 300 pA, 800–1000 mV for imaging butanethiol on Au(111) and highly irregular gold surfaces, and 25 pA, 1500 mV for AuNP supported on HOPG.

XPS measurements were performed with a Mg Kα source (1253.6 eV) from XR50, Specs GmbH and a hemispherical electron energy analyzer from PHOIBOS 100, Specs GmbH. Spectra were acquired with 10 eV pass energy and a Shirley type background was subtracted to each region. A two-point calibration of the energy scale was performed using sputtered cleaned gold (Au $4f_{7/2}$, binding energy = 84.00 eV) and copper (Cu $2p_{3/2}$, binding energy = 933.67 eV) samples. C 1s at 285 eV was used as charging reference. Electrodesorption curves were performed in a conventional 3-electrode glass cell filled with deareated 0.1 M NaOH aqueous solution. A high area platinum foil and a saturated calomel electrode (SCE) were used as counter and reference electrodes, respectively.

3. Thiol SAM structural aspects and thiol stability on different gold substrates

3.1. Planar surfaces

Planar gold substrates for thiol self-assembly include single crystals (commonly the (111) face) [25], and thin films supported on glass, mica or silicon prepared by physical vapor deposition (PVD), electrodeposition, or electroless deposition. Annealing of the evaporated films results in smooth polycrystalline films consisting of micrometer sized grains with (111) preferential orientation, suitable for molecular resolution using scanning tunneling microscopy (STM) or atomic force microscopy (AFM) [2, 26]. SAM formation on evaporated substrates or Au(111) single crystals takes place after exposure of several hours, or even days, to alkanethiols either in gas phase, by dosing the vapors in a vacuum chamber, or in liquid phase, by immersing the substrates in pure alkanethiol or in alkanethiol solutions [2, 8]. In the latter case, solvents of different polarities are used, like ethanol (the most important one), methanol, toluene and even water, depending on the thiol terminal group.

It has been reported that, for Au(111) single crystals and (111) preferred oriented flame annealed evaporated thin films, the self-assembly process involves the lifting of the well-known $22 \times \sqrt{3}$ herringbone reconstruction of the (111) surface and the formation of different alkanethiol lattices that evolve with adsorption time or thiol dose from lying down monolayers (or 'stripe' phases) to stable and dense monolayers of molecules in a near standing up configuration [26, 27].

Two different stable, dense surface structures have been observed by several surface science techniques, either from vapor or solution deposition: the $\sqrt{3} \times \sqrt{3}$R30° lattice [28] and its c(4 × 2) superlattices [4, 8, 29]. STM images taken for butanethiol $\sqrt{3} \times \sqrt{3}$R30° and c(4 × 2) superlattice domains on a flame annealed evaporated polycrystalline gold substrate are shown in figures 1(a) and (b). These and many others surface structures of alkanethiols on Au(111) have been described in several reviews [8, 9, 26]. Both structures have a surface coverage $\theta = 1/3$ and distances of ≈0.5 nm between nearest neighbor molecules. Three angles (figure 1(c)) fully describe the orientation of the thiol molecules for dense thiol SAMs on Au(111): α (the tilt angle with respect to the surface normal), β (the hydrocarbon chain twist angle) and χ (the precession angle). For the simpler $\sqrt{3} \times \sqrt{3}$R30° lattice [28], α results in 30°, β is 40°–55° and χ is 15°.

In particular, different models have been proposed to interpret the c(4 × 2) lattice, which propose different β values, or distances between S heads smaller than 0.5 nm, among others [30–32]. The $\sqrt{3} \times \sqrt{3}$R30° and c(4 × 2) lattices can coexist on the Au substrate forming separate domains, and their relative amount depends on the hydrocarbon chain length and on the preparation conditions [26]. Also, it is important to note that SAMs on flat gold terraces always present some defects, like pinholes, or domain boundaries, which can be preferred paths for charge transfer in aqueous solutions [33, 34].

Although these systems have been extensively studied, there is still controversy about some fundamental structural aspects. First, there is disagreement about the preferred adsorption site in the $\sqrt{3} \times \sqrt{3}$R30°: whereas most DFT calculations propose fcc or bridge-fcc sites [35], some recent experimental results have pointed that adsorption would occur at on-top sites [36–38], Also, the position of the sulfur heads in the c(4 × 2) lattice and the interpretation of the STM images for these lattices is under debate [29–32]. Very recently, the possibility of some sort of substrate reconstruction after the lifting of the $22 \times \sqrt{3}$, either for the lying down phases [39], or for the denser $\sqrt{3} \times \sqrt{3}$R30° and c(4 × 2) structures, has been proposed [40, 41]. Certainly, structural aspects for thiol SAMs on planar gold surfaces should be further investigated.

The thermodynamics of the adsorption process has also been studied, although there are still some doubts about the chemical reaction that takes place during the adsorption, both in gas phase and in solution [2, 42]. Even if reaction

$$\mathrm{RSH} + \mathrm{Au} = \mathrm{RS} - \mathrm{Au} + \tfrac{1}{2}\mathrm{H_2} \qquad (1)$$

is generally accepted for gas phase self-assembly, the formation of H_2 has not been experimentally detected. In aqueous solutions, water and other species could also be formed. In any case, what is known from experimental data and from DFT calculations is that the Au–S bond is strong (≈50 kcal mol^{-1}) [8].

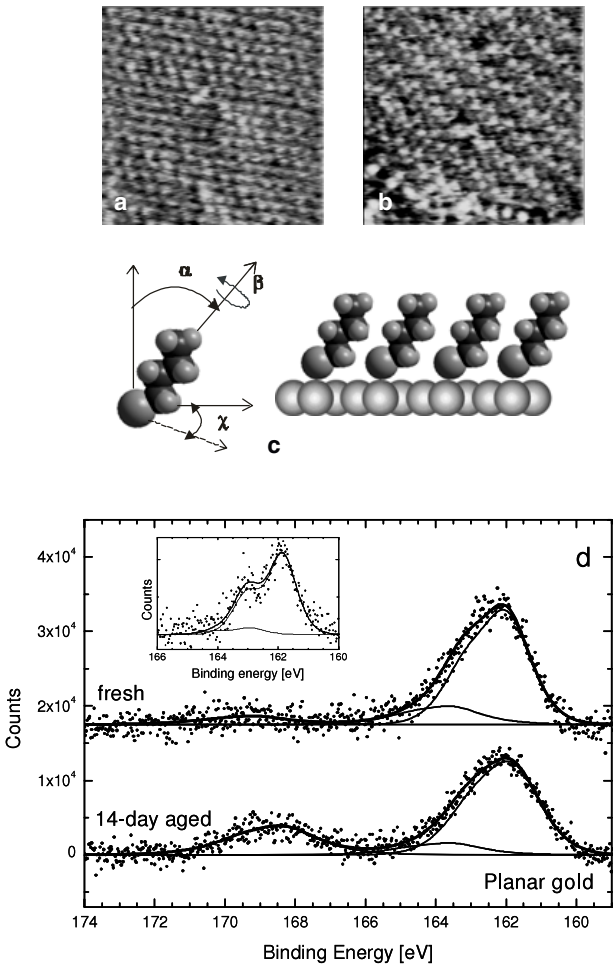

Figure 1. ((a) and (b)) STM images (top view) taken in air for a butanethiol SAM on Au(111). (a) 8 × 8 nm^2 STM image of the $\sqrt{3} \times \sqrt{3}$R30° lattice. (b) 8 × 8 nm^2 STM image of the c(4 × 2) lattice. (c) Schemes showing thiol molecules on Au (lateral view) and the three angles that define the thiol molecule orientation (α, β and χ). (d) XPS S 2p signals for a butanethiolate-covered Au(111). (upper) freshly prepared SAM, (lower) the same sample after a two-week exposure to ambient conditions. The inset shows the typical doublets of the S 2p components.

On the other hand, XPS measurements give valuable information about the chemical bonding of the S head to the Au surface [43–45]. In fact, the S 2p core level region for alkanethiol SAMs on a variety of metals can be fitted with different components. Figure 1(d) upper shows the XPS spectrum for a butanethiolate SAM on a flame annealed evaporated Au(111) substrate recorded immediately after SAM preparation. The $2p_{3/2}$ peak can be fitted with two components, with average binding energy values 162 and 163–164 eV, as observed in figure 1(d). Spectra taken at higher resolution (figure 1(d) inset) show that each component consists of a doublet with spin–orbit splitting of 1.2 eV. The component at 162 eV is usually the most important one and is related to S chemisorbed on the Au surface through a thiolate bond [46]. The minor component at 163–164 eV, corresponding to

unbounded thiol (or thiols in multilayers) [43], is typical for SAMs prepared from solution. This contribution decreases after careful sample rinsing with the solvent. Sometimes a third component at 161 eV is also observed, which has been attributed to adsorbed sulfide, present as a contaminant in the SAM [44, 46].

Recently, there has been much interest in the oxidative chemistry of SAMs. It is known that SAMs are damaged by secondary electrons, by x-rays (mainly due to photoelectrons), and also by ions and neutrals [20, 47, 48]. Although in general SAMs exhibit remarkable chemical stability, there has been some concern about their possible oxidation by ozone produced by UV irradiation [20], because of the drawback this would represent for many alkanethiol SAM applications, and also for the possible implications in nanophotolithography. The mercaptan groups yield alkyl sulfinates and sulfonates when exposed to strong oxidants like ozone. Photo-oxidation and photo-reduction have been observed in 8-chlorooctyldisulfide SAMs adsorbed on Au [49]. Oxidation at the Au/sulfur interface exposed to an ambient environment of light and air was observed by XPS, but no evidence was found for a similar sample kept in the dark with the exclusion of air. Experimental evidence suggests that photo-oxidation is mediated by the Au surface [50]. Although ozone has been assigned as the main species responsible for the S head oxidation in SAMs on metals [51], it has also been shown that SAM oxidation on exposure to UV light sources can occur in the absence of ozone [48]. Thus, while exposure to ozone does cause oxidation, it is not a necessary condition for SAM oxidation: hot electrons, formed by the absorption of photons by electrons in the substrate, are the most likely oxidation cause in this case.

The kinetics of oxidation varies depending on the morphology of the underlying gold. It has been reported that the rate of oxidation increases dramatically with the decrease in the grain size and the decrease of the amount of Au(111) on the surface [20], suggesting that thiol oxidation could be enhanced at interfacial grain boundaries of the Au films.

Degradation of the SAMs in ambient conditions by oxidation can be followed in time by XPS. In fact, S 2p components that correspond to weakly adsorbed alkyl sulfonates and other oxidized sulfur species resulting from the oxidation of the sulfur head are detected at binding energies $>$167 eV [20, 52].

The S 2p signal for the freshly prepared butanethiol SAM shown in figure 1(d) (upper) indicates a small amount of oxidized S species. However, the same SAM, after a two-week exposure to air in ambient conditions (room temperature and artificial light), shows a significant increase in the S 2p signal related to oxidized S species (figure 1(d), lower). This is a clear evidence of SAM degradation for planar preferred oriented Au(111) substrates.

3.2. Curved surfaces: nanoparticles

Gold nanoparticles (AuNP), and small metallic clusters in general, have been much studied in the last years because of their many potential applications and also because, as the NP size becomes smaller, some very interesting physical properties appear, due to quantum size and surface effects, which can be very different from those of the bulk metals [53, 54]. In fact, these nanostructures exhibit interesting properties, such as magnetism [55, 56], novel surface reactivity [57], and electromagnetic energy localization as seen in plasmon absorption spectra [54], some of which can be attributed to quantum size effects.

There are several methods for AuNP preparation, like the old Turkevich procedure using citrate, the Brust method for thiol-capped NP, and others using hydrosols, polymers (like PVD), etc [10, 15, 58–60]. In all cases the average size of the NP can be controlled by changing the ratio of reducing agent to gold salt, or the temperature, among other variables.

In the Brust method (and others related) alkanethiols play a crucial role during the synthesis of AuNP, by reducing their growth rate and stabilizing them against aggregation [2, 59]. Thiols have been widely used as molecular anchors to functionalize metal NP with different kinds of molecules, biomolecules and nanostructures, by simply choosing an appropriate terminal group [16] and using different immobilization methods (covalent attachment, physisorption, etc). Therefore, thiol capping of nanoparticles has a double function. Moreover, the S–Au bond of thiol-capped nanoparticles has been associated to some unique physical properties of these nanostructures, like permanent magnetism, which is not found for AuNP with similar size but stabilized by means of a surfactant, or for bulk Au [61].

AuNP formed in the presence of alkanethiols adopt a quasi-spherical shape because they have similar affinities for the low-index crystal faces [62], so that thiols are not suitable to synthesize nanostructures like nanoprisms or nanorods. AuNP larger than 0.8 nm are believed to have a truncated octahedral or cubo-octahedral shape, depending on the number of gold atoms in the core, with (111) faces truncated by smaller (100) faces [62], and, hence SAMs on AuNP can be, in principle, compared with those on planar gold surfaces.

Figure 2(a) shows an STM image of the butanethiol-capped AuNP supported on a highly oriented pyrolytic graphite substrate, while figure 2(b) shows a scheme of these nanoparticles on the substrate. The AuNP were adsorbed on the substrate by immersion in 0.3 mg ml^{-1} AuNP-containing hexane solution for 30 min. While the Au core of these NP is 2.9 nm, the NP size including the butanethiol cap is $\approx$4 nm.

For NP with Au cores smaller than 5 nm, a great number of atoms are located at the nanoparticle surface. The number of surface atoms and the curvature decrease sharply as the NP size increases, reaching bulk properties for sizes larger than 10 nm. A large number of Au surface atoms are located at corners and edges of NP: in fact, for NP 1–2 nm in size 45% of all surface atoms are located at these defective sites [2, 62]. The greater concentration of atoms at surface defects and the high radius of curvature of the cluster allow a larger proportion of the Au atoms to be on the cluster surface, which in turn results in a greater coverage of the thiol monolayer on the surface [63–66]. EXAFS data suggest that NP smaller than 5 nm have almost twice S ($\theta = 2/3$) as found on planar surfaces ($\theta = 1/3$) [63, 64]. XPS data (figure 2(c) upper) for

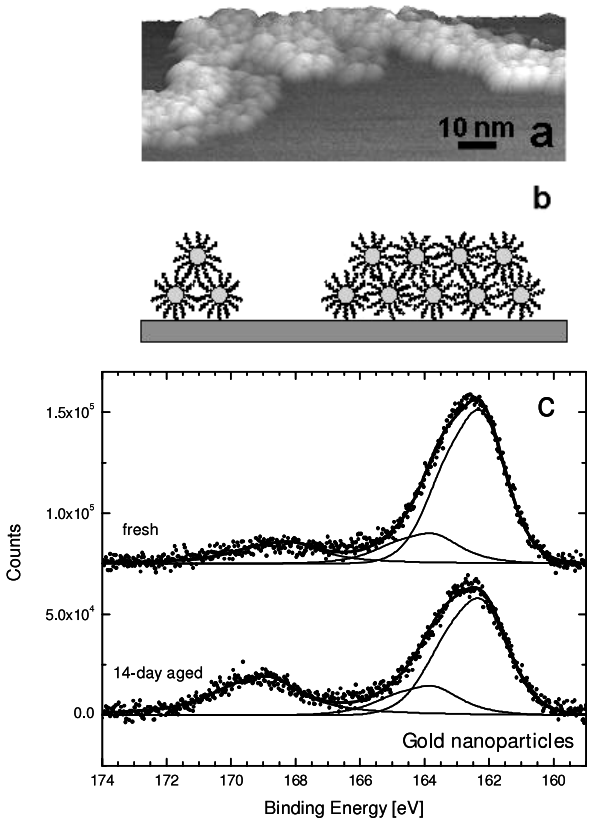

Figure 2. (a) 114 × 114 nm^2 STM image of butanethiol-capped AuNPs 2.9 nm core in size adsorbed on HOPG, (b) scheme showing the thiol-capped AuNP on the substrate. (c) XPS S 2p signals for the freshly (upper) and aged in air (lower) AuNP on HOPG.

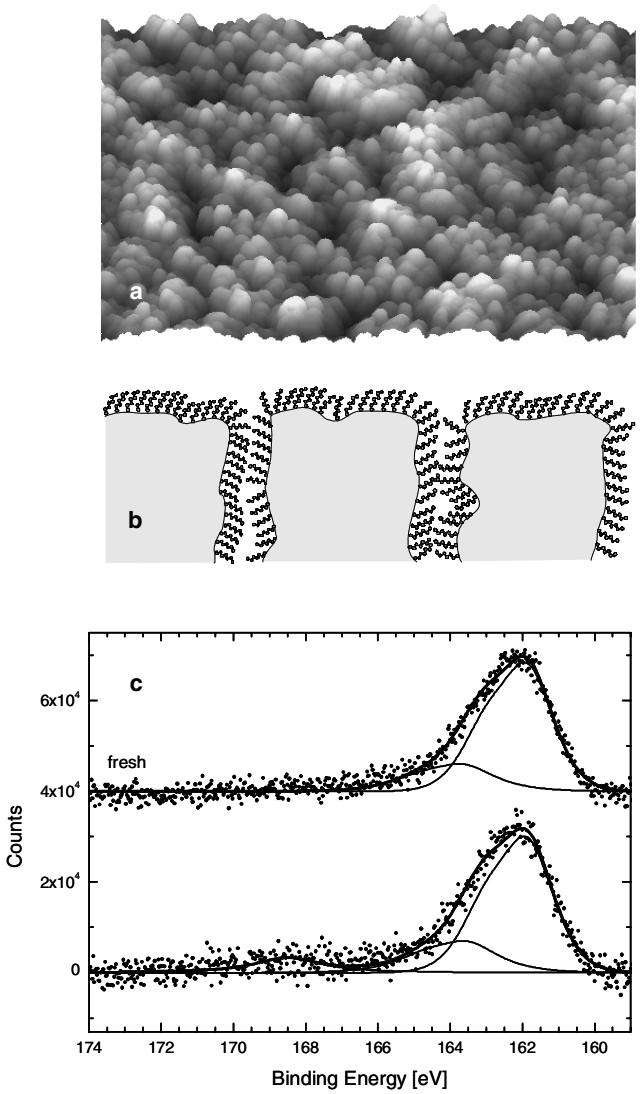

Figure 3. (a) 620 × 620 nm^2 STM image (3D view) of a butanethiol-covered nanostructured high area Au surface. The average grain size is 12 nm. (b) Scheme showing the structure of the thiol-covered nanostructured substrate (lateral view). (c) XPS S 2p signals for a butanethiol-covered nanostructured high area Au substrate. Upper: freshly prepared SAM; lower: the same sample after two-week exposure to ambient conditions.

carefully cleaned butanethiol-capped AuNP (2.9 nm core size) adsorbed from hexane on graphite are consistent with these observations. Also in this case the S 2p signal can be fitted with two components at 162.5 and 163–164 eV, corresponding to chemisorbed S as a thiolate and unbounded thiols, respectively. Again, chemisorbed thiolates dominate the spectrum, while only a trace of unbounded thiols is observed. An estimation of the amount of chemisorbed S, taking into account the S/Au ratio and the attenuation factor, yields larger thiol coverage for AuNP than for planar Au.

A large amount of unbounded molecules has been observed by XANES on AuNP covered by long alkanethiols [63]. Actually, a consequence of the high curvature radius is the decrease in the chain density as one moves away from the NP surface. The open outer structure enhances interdigitation with chains of free thiols. Careful cleaning of the NP with hexane or ethanol results in the decrease of the 163–164 eV component in the XPS spectra.

Moreover, as observed for planar surfaces, a long-time exposure to air (two weeks) of the AuNP supported on HOPG results in a significant increase in the amount of oxidized S species that appear at binding energies >167 eV (figure 2(c)). It should be noted that this degradation takes place when supported on the HOPG surface. In fact, the two week time refers to the time period when the AuNP were exposed to ambient conditions on the HOPG surface. On the other hand, AuNPs kept in hexane or as a dry powder exhibit no oxidation signals for long periods of time (they can be stored for months).

3.3. Irregular surfaces: nanostructured high area Au layers

Irregular high area metallic surfaces can be prepared by physical, chemical and electrochemical methods [24]. In particular, nanostructured high area Au layers can be easily prepared by fast electroreduction of thick hydrous AuO produced by anodization of polycrystalline Au in acid medium (see section 2). The resulting surfaces consist of nanosized grains and pores of micrometric depth, as shown in figures 3(a) and (b).

An accurate way to estimate the total amount of chemisorbed thiol species in these complex surfaces is by

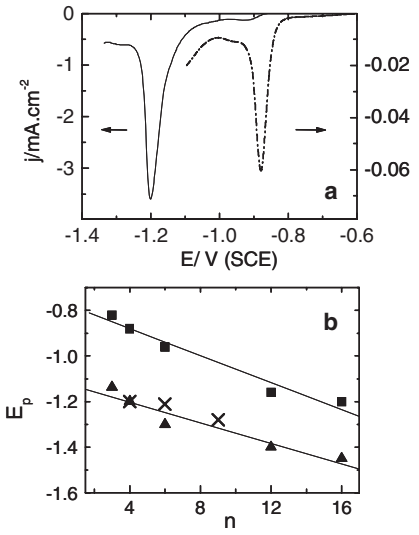

Figure 4. (a) Current density (j) versus potential (E) curves recorded at 0.05 V s^{-1} for butanethiol SAMs on planar (dashed line) and nanostructured high area Au substrates (solid line), with j referred to the geometric substrate area. The current peaks correspond to thiol desorption. (b) E_p versus n plots for thiol SAMs on different substrates. (■) planar gold, (×) gold nanoparticles, (▲) nanostructured high area gold.

desorbing the thiol in alkaline solutions by means of linear voltammetry [19]. On the other hand, XPS can only give information of a thin 2–3 nm layer in the outer part of the porous Au with a thickness in the micrometer range.

Figure 4(a) shows typical electrodesorption (j/E) curves in a 0.1 M NaOH aqueous solution for butanethiol-covered planar and nanostructured high area Au. The current peaks in the curves are related to the reductive desorption of thiols from the Au substrates, according to reaction [67, 68]

$$\mathrm{RS-Au + e = RS^- + Au.} \qquad (2)$$

The charge density (q), measured by integration of the current peaks shown in figure 4(a) and referred to the real surface area, yields 75 ± 8 μC cm^{-2}, a result that corresponds to $\theta \approx 1/3$ for both planar and irregular surfaces [19]. Therefore, neither excluded volume effects (that would result in a decrease in q), nor curvature effects (that would result in an increase in q) are significant for thiols on these irregular surfaces.

XPS data show that thiols are also chemisorbed on these highly irregular surfaces (S $2p_{3/2}$ component at 162 eV) (figure 3(c) upper). The S/Au ratio is 80% higher than on planar surfaces, i.e. more S is detected by XPS on the irregular surfaces, due to the volume sampled by the photoelectrons. We also observe only traces of SAM degradation to yield oxidized S species (figure 3(c), lower). Contrary to other reported results for polycrystalline gold surfaces (yet not nanoporous) [20], we have found an enhanced stability in air of the SAMs on these complex nanostructured substrates, as compared to planar gold substrates and to AuNP. In fact, a comparison of the XPS data for the different substrates (see figures 1(c), 2(c), 3(c)) indicates that the oxidation rate in air increases in the following order: irregular gold < planar gold ≈ supported nanoparticles. This is an interesting result that deserves further investigation and that could open new insight for the long-time applications of thiol SAMs on gold. In fact, SAM degradation in ambient conditions is one of the most important drawbacks for the use of these organic films for some nanotechnological applications.

It should be mentioned that, as in the case of AuNP, the formation of a thiol SAM can stabilize the nanostructured system [19]. Actually, after their preparation, the irregular Au deposits decrease their surface area in order to decrease their surface free energy following a $r \propto t^{-4}$ relationship, where t is time and r is the radius of the nanoparticle [69]. This process, which results in grain growth from the nanoscale to the microscale, is produced by mass transport of Au adatoms from smaller to larger grains. Adsorbed alkanethiols hinder the surface diffusion of Au adatoms by thiol–substrate and thiol–thiol interactions, and allow the Au nanostructures to almost keep their initial surface area.

3.4. Comparison of the stability of thiol molecules in aqueous media on the different gold surfaces

The peak potential (E_p) of the j/E curves shown in figure 4(a) gives information about the stability of thiol molecules on the Au substrates in aqueous environments [67, 68]. Thiol stability in aqueous environments is crucial for many applications in material and biological sciences. It is well known that thiols desorb from metallic electrodes and that the desorption potential becomes more negative as the number of C atoms (n) increases, due to the stabilizing effect of van der Waals interactions and also to hydrophobic forces. In figure 4(b) we have plotted E_p versus n for thiol SAMs on planar Au substrates, AuNP, and nanostructured high area surfaces. As expected, E_p moves toward more negative values as the length of the thiol hydrocarbon chain is increased, irrespective of the type of substrate structure. The slopes of the E_p versus n plots are 3 and 2.5 kJ mol^{-1} per C atom of the hydrocarbon chain for planar substrates, and for the nanocurved and irregular Au substrates, respectively. These values suggest that the irregular nature of the substrate surface does not introduce significant differences in the intermolecular forces acting at SAMs. The slight decrease could be assigned to the disorder introduced by the curved and irregular substrates on the SAM, which precludes the optimization of the hydrocarbon chain–hydrocarbon chain interactions. Figure 4(b) also reveals that, for the same thiol, electrodesorption from the irregular and nanocurved surfaces takes place at more negative potential values, i.e. more energy is needed to remove thiols from these surfaces than from planar surfaces. We can speculate that the large number of non-coordinated sites of the defective surfaces allows a stronger chemisorption of the S head to the Au surface, resulting in a shift of the peak potential to more negative values [23, 70]. In fact, *in situ* STM images have shown that, after S [71] and thiol [72] electrodesorption from terraces occurs, S species still remain adsorbed at step edges of the Au(111) surfaces.

4. Conclusions

Thiol SAMs on surfaces of nanoparticles smaller than 10 nm (like thiol-capped AuNP) present features different to those of planar gold substrates due to curvature effects and to the large density of substrate defects. These facts result in a higher surface coverage and stronger thiol–substrate adsorption than for planar gold surfaces. For porous nanostructured surfaces with particle sizes >10 nm, the large defect density also results in stronger thiol–substrate bonds but a similar surface coverage, since curvature effects vanish in this scale. The stability against air of thiols chemisorbed on irregular nanostructured Au is increased with respect to planar Au surfaces and AuNP. Therefore, high area nanostructured Au surfaces can be promising platforms for the preparation of dense and stable SAMs in air or in electrolyte solutions.

Acknowledgments

This work was supported by the Agencia Nacional de Promoción Científica y Tecnológica (PICT 02-11111 and PICT 05-632439) and CONICET (PIP 0675). MEV is a member of the research career division of CIC-Bs As. The authors acknowledge Professors F Requejo and Y S Shon for providing the thiol-capped Au nanoparticles.

References

[1] Castner D G and Ratner B D 2002 *Frontiers in Surface and Interface Science* ed C B Duke and E W Plummer (Amsterdam: North-Holland)
[2] Love J C, Estroff L A, Kriebel J K, Nuzzo R G and Whitesides G M 2005 *Chem. Rev.* **105** 1103
[3] Wilbur J L and Whitesides G M 1999 *Nanotechnology* ed G Timp (New York: Springer)
[4] Gates B D, Xu Q, Stewart M, Ryan D, Grant Wilson C and Whitesides G M 2005 *Chem. Rev.* **105** 1171
[5] Kushmerick J G, Pollack S K, Yang J C, Naciri J, Holt D B, Ratner M A and Shashidhar R 2003 *Ann. New York Acad. Sci.* **1006** 277
[6] Cunningham A 1998 *Introduction to Bioanalytical Sensors* (New York: Wiley–Interscience)
[7] Ulman A 1996 *Chem. Rev.* **96** 1533
[8] Schreiber F 2000 *Prog. Surf. Sci.* **65** 151
Schreiber F 2004 *J. Phys.: Condens. Matter* **16** R881
[9] Vericat C, Vela M E, Benitez G A, Martin Gago J A, Torrelles X and Salvarezza R C 2006 *J. Phys.: Condens. Matter* **18** R867–900
[10] Daniel M-C and Astruc D 2004 *Chem. Rev.* **104** 293
[11] Shenhar R and Rotello V M 2003 *Acc. Chem. Res.* **36** 549–61
[12] Gittins D I, Bethell D, Schiffrin D J and Nichols R J 2000 *Nature* **408** 67
[13] Rosi N L, Giljohann D A, Thaxton C S, Lytton-Jean A K R, Han M S and Mirkin C A 2006 *Science* **312** 1027
[14] Baron R, Onopriyenko A, Katz E, Lioubasheski O, Willner I, Wang S and Tian H 2006 *Chem. Commun.* **20** 2147–9
Beissenhirtz M K, Elnathan R, Weizmann Y and Willner I 2007 *Small* **3** 375
[15] Cushing B L, Kolesnichenko L and O'Connor C J 2004 *Chem. Rev.* **104** 3893
[16] Templeton A C, Hostetler M J, Warmoth E K, Chen S, Hartshorn C M, Krishnamurthy V M, Forbes M D E and Murray R W 1998 *J. Am. Chem. Soc.* **120** 4845
[17] Eggins B 1999 *Biosensors: An Introduction* (Chichester: Wiley)
[18] Notsu H, Kubo W, Shitanda I and Tatsuma T 2005 *J. Mater. Chem.* **15** 1523
[19] Vericat C, Benitez G-A, Vela M E, Salvarezza R C, Tognalli N-G and Fainstein A 2007 *Langmuir* **23** 1152
[20] Lee M T, Hsueh C C, Freund M S and Ferguson G S 1998 *Langmuir* **14** 6419
[21] Andreasen G, Vela M E, Salvarezza R C and Arvia A J 1997 *Langmuir* **13** 6814
[22] Brust M, Walker M, Bethell D, Schiffrin D J and Whyman R 1994 *Chem. Commun.* **40** 801
[23] Grumelli D, Vericat C, Benitez G, Vela M E, Salvarezza R C, Ramallo-Lopez J M, Requejo F A, Craievich A F and Shon YS 2007 *J. Phys. Chem.* C **111** 7179
[24] Salvarezza R C and Arvia A J 1996 *Modern Aspects of Electrochemistry* (New York: Plenum) chapter 5
[25] Poirier G E and Pylant E D 1996 *Science* **272** 1145
[26] Vericat C, Vela M E and Salvarezza R C 2005 *Phys. Chem. Chem. Phys.* **7** 3258
[27] Widrig C A, Alves C A and Porter M D 1991 *J. Am. Chem. Soc.* **113** 2807
Dubois L H, Zegarski B R and Nuzzo R G 1993 *J. Chem. Phys.* **98** 678
[28] Fenter P, Eisenberger P and Liang K S 1993 *Phys. Rev. Lett.* **70** 2447
Camillone N III, Chidsey C D E, Liu G-Y and Scoles G 1993 *J. Chem. Phys.* **98** 3503
[29] Anselmetti D, Baratoff A, Güntherodt H J, Delamarche E, Michel B, Gerber C, Kang H, Wolf H and Ringsdorf H 1994 *Europhys. Lett.* **27** 365
[30] Terán Arce F, Vela M E, Salvarezza R C and Arvia A J 1998 *J. Chem. Phys.* **109** 5703
[31] Fenter P, Eberhardt A and Eisenberger P 1994 *Science* **266** 1216
[32] Torrelles X, Barrena E, Munuera C, Rius J, Ferrer S and Ocal C 2004 *Langmuir* **20** 9396
[33] Vericat C, Remes Lenicov F, Tanco S, Andreasen G, Vela M E and Salvarezza R C 2002 *J. Phys. Chem.* B **106** 9114
[34] Benítez G, Vericat C, Tanco S, Remes Lenicov F, Castez M F, Vela M E and Salvarezza R C 2004 *Langmuir* **20** 5030
[35] Beardmore K M, Kress J D, Grønbech-Jensen N and Bishop A R 1998 *Chem. Phys. Lett.* **286** 40
Grönbeck H, Curioni A and Andreoni W 2000 *J. Am. Chem. Soc.* **122** 3839
Andreoni W *et al* 2000 *Int. J. Quantum Chem.* **80** 598
Yourdshahyan Y, Zhang H K and Rappe A M 2001 *Phys. Rev.* B **63** 081405R
Vargas M C, Giannozzi P, Selloni A and Scoles G 2001 *J. Phys. Chem.* B **105** 9509
Hayashi T, Morikawa Y and Nozoye H 2001 *J. Chem. Phys.* **114** 7615
Akinaga Y, Nakajima T and Hirao K 2001 *J. Chem. Phys.* **114** 8555
Gottschalck J and Hammer B 2002 *J. Chem. Phys.* **116** 784
Yourdshahyan Y and Rappe A 2002 *J. Chem. Phys.* **117** 825
Franzen S 2003 *Chem. Phys. Lett.* **381** 315
Molina N M and Hammer B 2002 *Chem. Phys. Lett.* **360** 264
Tachibana M, Yoshizawa K, Ogawa A, Fujimoto H and Hoffmann R 2002 *J. Phys. Chem.* B **106** 12727
Cometto F P, Paredes-Olivera P, Macagno V A and Patrito E M 2005 *J. Phys. Chem.* B **109** 21737
[36] Kondoh H, Iwasaki M, Shimada T, Amemiya K, Yokoyama T, Ohta T, Shimomura M and Kono S 2003 *Phys. Rev. Lett.* **90** 066102
[37] Roper M G, Skegg M P, Fisher C J, Lee J J, Dhanak V R, Woodruff D P and Jones R G 2004 *Chem. Phys. Lett.* **389** 87
[38] Torrelles X, Vericat C, Vela M E, Fonticelli M H, Daza Millone M A, Felici R, Lee T-L, Zegenhagen J, Muñoz G, Martín-Gago J A and Salvarezza R C 2006 *J. Phys. Chem.* B **110** 5586

[39] Maksymovych P, Sorescu D C and Yates J T Jr 2006 *Phys. Rev. Lett.* **97** 146103
[40] Yu M, Bovet N, Satterley C J, Bengio S, Lovelock K R J, Milligan P K, Jones R G, Woodruff D P and Dhanak V 2006 *Phys. Rev. Lett.* **97** 166102
[41] Mazzarello R, Cossaro A, Verdini A, Rousseau R, Casalis L, Danisman M F, Floreano L, Scandolo S, Morgante A and Scoles G 2007 *Phys. Rev. Lett.* **98** 016102
[42] Zhong C-J, Woods N T, Brent Dawson G and Porter M D 1999 *Electrochem. Commun.* **1** 17
[43] Castner D, Hinds K and Grainger D W 1996 *Langmuir* **12** 5083
[44] Ishida T, Hara M, Kojima I, Tsuneda S, Nishida N, Sasabe H and Knoll W 1998 *Langmuir* **14** 2092
[45] Zhong C-J, Brush R C, Anderegg J and Porter M D 1999 *Langmuir* **15** 518
[46] Vericat C, Vela M E, Andreasen G, Salvarezza R C, Vázquez L and Martín-Gago J A 2001 *Langmuir* **17** 4919
[47] Heister K, Zharnikov M, Grunze M, Johansson L S O and Ulman A 2001 *Langmuir* **17** 8
[48] Feulner P, Niedermayer T, Eberle K, Schneider R, Menzel D, Baumer A, Schmich E, Shaporenko A, Tai Y and Zharnikov M 2005 *Surf. Sci.* **593** 252
[49] Brewer N J, Rawsterne R E, Kothari S and Leggett G J 2001 *J. Am. Chem. Soc.* **123** 4089
[50] Rieley H, Price N J, Smith T L and Yang S 1996 *J. Chem. Soc. Faraday Trans.* **92** 3629
[51] Ferris M M and Rowlen K L 2000 *Appl. Spectrosc.* **54** 664
[52] Wirde M, Gelius U and Nyholm L 1999 *Langmuir* **15** 6370
[53] Zhang P and Sham T K 2003 *Phys. Rev. Lett.* **90** 245502
[54] Rao C N R, Kulkarni G U, Thomas P J and Edwards P P 2002 *Chem. Eur. J.* **8** 28
[55] Yamamoto Y and Hori H 2006 *Rev. Adv. Mater. Sci.* **12** 23
[56] De La Venta J, Pinel E F, Garcia M A, Crespo P, Hernando A, De La Fuente R, De Julián Fernández C, Fernández A and Penadés S 2007 *Mod. Phys. Lett.* B **21** 303
[57] Campbell C T 2004 *Science* **306** 234
Chen M S and Goodman D W 2004 *Science* **306** 252
Davis R J 2003 *Science* **301** 926
[58] Frens G 1973 *Nature (Phys. Sci.)* **241** 20
[59] Brust M, Walker M, Bethell D, Schiffrin D J and Whyman R 1994 *J. Chem. Soc. Chem. Commun.* **80** 801
[60] Drechster U, Erdogan B and Rotello V M 2004 *Chem. Eur. J.* **10** 5570
[61] Crespo P, Litran R, Rojas T C, Multigner M, de la Fuente J M, Sánchez-López J C, García M A, Hernando A, Penadés S and Fernández A 2004 *Phys. Rev. Lett.* **93** 087204
[62] Templeton A C, Wuelfing W P and Murray R W 2000 *Acc. Chem. Res.* **33** 27
Gutierrez-Wing C, Ascencio J A, Perez-Alvarez M, Marin-Almazo M and Jose-Yacaman M 1998 *J. Cluster Sci.* **9** 529
Luedtke W D and Landman U 1996 *J. Phys. Chem.* **100** 13323
Luedtke W D and Landman U 1998 *J. Phys. Chem.* B **102** 6566
[63] Ramallo-López J M, Giovanetti L J, Requejo F G, Isaacs S R, Shon Y S and Salmeron M 2006 *Phys. Rev.* B **74** 073410
[64] Pradeep T and Sandhyarani N 2002 *Pure Appl. Chem.* **74** 1593
[65] Jadzinsky P D, Calero G, Ackerson C J, Bushnell D A and Kornberg R D 2007 *Science* **318** 430
[66] Zanchet D, Tolentino H, Martins Alves M C, Alves O L and Ugarte D 2000 *Chem. Phys. Lett.* **323** 167
[67] Vela M E, Martin H, Vericat C, Andreasen G, Hernández Creus A and Salvarezza R C 2000 *J. Phys. Chem.* B **104** 11878
[68] Azzaroni O, Vela M E, Andreasen G, Carro P and Salvarezza R C 2002 *J. Phys. Chem.* B **106** 12267
[69] Barabasi A L and Stanley H E 1995 *Fractal Concepts in Surface Growth* (Cambridge: Cambridge University Press)
[70] Leibowitz F L, Zheng W, Maye M M and Zhong C 1999 *J. Anal. Chem.* **71** 5076
[71] Vericat C, Andreasen G, Vela M E and Salvarezza R C 2000 *J. Phys. Chem.* B **104** 302
[72] Vericat C, Andreasen G, Vela M E, Martín H and Salvarezza R C 2001 *J. Chem. Phys.* **115** 6672